https://doi.org/10.1016/j.nanoen.2018.11.014

Piezophotonic Effect Based on Mechanoluminescent Materials for Advanced Flexible Optoelectronic Applications

Xiandi Wang[a,c,1], Dengfeng Peng [b,1], Bolong Huang [d], Caofeng Pan [a,b,c,*], Zhong Lin Wang [a,c,e]

[a] *CAS Center for Excellence in Nanoscience, Beijing Key Laboratory of Micro-nano Energy and Sensor, Beijing Institute of Nanoenergy and Nanosystems, Chinese Academy of Sciences, Beijing 100083, P. R. China*

[b] *College of Optoelectronic Engineering, Shenzhen University, Shenzhen, 518060, China*

[c] *School of Nanoscience and Technology, University of Chinese Academy of Sciences, Beijing 100049, P. R. China*

[d] *Department of Applied Biology and Chemical Technology, The Hong Kong Polytechnic University, Hung Hom, Kowloon, Hong Kong, China*

[e] *School of Materials Science and Engineering, Georgia Institute of Technology, Atlanta, Georgia30332-0245, USA*

* Corresponding author.
E-mail address: cfpan@binn.cas.cn (C. F. Pan).

[1] These authors contributed equally to this work.

Keywords: piezophotonic effect, mechanoluminescence, flexible, optoelectronic

Abstract

Recently, there has been an increasing research interest in the emerging fields of piezophotonics, which is the great interesting physics responsible for numbers of important technologies such as light source, smart sensor and mechanoelectronics. Piezophotonic effect is the coupling between the piezoelectric polarization and the photonic excitation in crystal that has a non-central symmetry. The strain-induced piezopotential can stimuli the photon emission without additional energy excitation such as light and electricity, which also offers great new opportunities of manipulating and fabrication of flexible optoelectronic devices. In this review, we will give a detailed description of the piezophotonic effect including its theoretical fundamental and practical applications. The piezophotonic light emission in doped ZnS CaZnOS, $SrAl_2O_4$ and $LiNbO_3$ attract great interesting during the past years, and researchers have executed many scientific inquiries into flexible/stretchable optoelectronic devices. Until now, significant breakthroughs have been achieved on piezophotonic e-signature system, visible wearable electronic devices and multi-physical coupling devices. Certainly, rapid innovations in this field will be quite significant to the future of human life.

1 Introduction

With the development of the advanced material science and optoelectrical technology, numbers of electronic devices are becoming increasingly functionalized, miniaturize and intellectual [1-6]. Searching for renewable and functional materials that possessing two or more desirable properties in a single entity have attracted broad interest. During the past decades, researchers from physics and material science have been keeping continuous interest of exploring the properties of the materials for their integration and coupling effects.[7] Multifunctional functional materials such as porous silicon, magnetic semiconductor, piezoelectric semiconductor, multiferroeletrics, topological insulator, and graphene superconductor have been widely studied [8-14]. Among these functional materials, piezoelectric semiconductors have been drawn lots of attention for their great potential optoelectronic applications [15-18].

Piezoelectricity is an effect that the production of electrical potential in a substance as the pressure on it changes. The piezoelectric effect results from the linear electromechanical interaction between the mechanical and electrical states in crystalline materials with no inversion symmetry [19-21]. Piezoelectric materials both in the form of big single crystals/ceramics and nanostructures have uniquely electrical, mechanical, thermal and optical properties, which result in great important applications in optoelectronic devices [7].

In the past decades, piezoelectric semiconductors, especially II-VI and III-V compound with wurtzite structures, have been drawing increasing attention because of their interesting coupling physics and wide spread applications in photonics, electronics, sensors, and energy harvester [22-25]. By utilizing the advantages offered by their multiple functionalities of

piezoelectricity, semiconductor and photon excitation, an unprecedented new optoelectronic fields have been created by taking advantages of the piezopotential on the transport behavior of charge carriers [26, 27]. Electronics fabricated by using inner crystal piezopotential as a gate voltage to control the charge transport behavior is named piezotronics, which have large ranges of applications in mechanical stimulated electronic devices, sensors and logic units [28-30]. Piezo-phototronics is a new field that is coined using three-way coupling among piezoelectricity, photonic excitation and semiconductor transport, which can turn/control electro-optical processes by strain-induced piezopotential [31], and thus have been used in the applications of piezo-light emitting diode (LED), piezo-solar-cell, piezo-photon-detector, piezo-photon-catalysis [32-36]. In 2007 and 2010, Wang first introduced the fundamental principle of piezotronics and piezophototronics, respectively as shown in Fig 1 [22, 37]. In 2008, Wang summarized the fundamental principle piezophotonics as the two way couplings of piezoelectricity and photoexcitation [38]. Among the large numbers of piezoelectric materials, semiconductors e.g. ZnS and insulators e.g. $LiNbO_3$ have been reported to show magic light emission under the mechanical force.

This review focuses on the introduction of the piezophotonic effect for advanced flexible optoelectronic applications. The main contents include the following aspects: i) Theoretical fundamental of piezotronic effect and piezophotonic effect. The strain-induced piezopotential can stimuli the photon emission, which is the core content of the piezophotonic effect. ii) The introduction of flexible/stretchable optoelectronic devices based on the piezophotonic effect. Significant breakthroughs have been achieved on piezophotonic e-signature system, visible wearable electronic devices and multi-physical coupling devices. iii) Advances in

piezophotonics materials and future trends. We introduce several representative preparation process and materials, and summarize novel trends for visual electronic skin.

2 Fundamentals of Piezophotonics

2.1 Piezoelectricity and Piezopotential

Piezoelectricity is an effect that the generation of the electric charge is in response to applied pressure in certain solid materials, and thus has been extensively used in many fields such as electromechanical sensors, astronautics, communication, and so on [7]. Especially, certain semiconductor materials, such as ZnO, GaN, InN, and ZnS, not only have excellent semiconductor properties, but also possess piezoelectric properties due to their wurtzite-structure (non-centrally symmetric crystal structure) [22]. For example, ZnO has a hexagonal wurtzite structure, containing two interconnecting hexagonal closed packed sublattices of Zn^{2+} and O^{2-}, as shown in Fig. 2a [39]. Due to its non-central symmetry, it exhibits anisotropic properties in the directions along and perpendicular to the *c*-axis, which is also a key factor in crystal growth, etching and defect generation. On the other hand, each Zn^{2+} ion is tetrahedrally connected to O^{2-} ion, demonstrating the coinciding center of positive charges and negative charges, leading to the electric neutrality of the crystal under strain-free condition. Whereas, the centers of cations and anions are slightly separated along the *c*-axis under a stress applied on the top of the tetrahedron, resulting in the induction of a dipole moment. Hence, a macroscopic piezoelectric potential, piezopotential, is created along the straining direction in the crystal with the accumulation of all the units. This inner piezopotential makes it possible to tune or control the electronic transport properties across an interface/junction.

2.2 Piezotronic Effect

In 2006, Wang's group firstly demonstrated a piezoelectric field effect transistor in which the piezoelectric potential induced by the applied pressure worked as a gate voltage to drastically control the transport properties of charge carriers. Then, a series of systematical works and concepts were reported to explain piezotronic effect that the piezopotential can tune/control the charge transport characteristic across an interface/junction. Notably, the piezotronic effect on metal-semiconductor (M-S) contact and p-n junction, as two most fundamental structures in semiconductor devices, was deeply investigated for the theoretical and practical value [40, 41].

The metal-semiconductor contact is a common constitution in various kinds of semiconductor electronic devices. A Schottky barrier is induced at the M-S junction area by contacting a metal and a semiconductor if the electron affinity of the semiconductor is significantly smaller than the work function of the metal, as shown in Fig. 2b [37]. For an n-type semiconductor, electrons need extra potential energy ($e\phi_i$) to pass through the Schottky barrier ($e\phi_{SB}$). On the other hand, piezoelectric polarization charges are created under applied strain if the semiconductor also possesses piezoelectric property. Then, a negative or positive piezopotential at the M-S interface can effectively enhance or reduce the local Schottky barrier height to $e\phi'$. In other words, the piezotronic effect on M-S contact is that the strain-induced piezopotential at the interfacial region can effectively modulate the local contact properties, which can further tune/control the charge carrier transport process of the device.

Similarly, the piezopotential can also significantly change the local band structure on the

p-n junction. Indeed, a charge depletion zone will be created by contacting an n-type semiconductor with a p-type one to balance the local potential at the interfacial p-n junction, as depicted in Fig. 2c [31]. It's notable that such a carrier-free zone has a positive effect on the piezoelectric effect due to the maximal retention of the piezo-charges. Taking a p-n junction with piezoelectric n-type semiconductor as an example, the strain-induced negative piezo-charges at the interface can make the local band structure upward bend slightly. This bending band will be effective to trap more holes from the p-type semiconductor, resulting in the enhancement of the electron-hole recombination rate. Conversely, the strain-induced positive piezo-charges at the p-n junction create a dip in the local band structure, leading to the accumulation of electrons from the n-type side, and thus modify carrier transport characteristics. As discussed above, it's clear that the strain-induced piezopotential can modify the local band structure near the interfacial region so that to effectively tune/control the generation, separation, recombination, and transport of charge carriers [42-44].

2.3 Piezophotonic Effect

In 2008, Wang's group had designed and performed an experiment to investigate the lifetime of the piezopotential created in ZnO NW. It was found that the piezopotential had a positive influence on the strong trapping electrons in vacancy or surface states. Subsequently, it was pointed out that the strain-induced piezopotential might make these trapped charges drop to the valence band, leading to photon emission, which is also called piezophotonic effect [38]. Similarly, for a p-n junction, the electrons on the piezoelectric n-type semiconductor may drift to the p-type semiconductor for the electron-hole recombination with the assistance of the strain-induced piezopotential, thus realizing the photon emission, as

shown in Fig. 2c [37]. However, little relevant experimental data on the piezophotonic effect was obtained based on the ZnO NW due to some rigorous restriction conditions. For example, the induced piezopotential ($> \phi_i$) should be large enough to drive the electrons passing through the p-n junction. Then, charge carriers traverse the depletion zone in a time shorter than the time for the electron-hole recombination. Additionally, there should be enough carriers available within the field of piezoelectric potential.

On the other hand, one property of photonic materials is the photon emitting, which have been extensively investigated for century because of their interesting physics and widespread applications. As the photon emitting material, the types of light emission may be distinguished by the light excitation approach. Most of our well known light emission materials can be excited by photon and electricity, for instance, photoluminescence (PL) is excited by photon energy, and electroluminescence (EL) is stimulated by electric field. Different to the stimulation by photon and electric field, there is interesting photonic materials of which light emission can be directly excited by mechanical energy or namely mechanically-induced light emission materials. Since 2015, we are trying to systematically explore the piezophotonic effect based on the mechanoluminescent ZnS:Mn particles [45].

To better understand this mechanoluminescene (ML) process in ZnS:Mn, we introduced the piezophotonic effect, strain-induced photon emission, to give a possible explanation with the energy band theory, as showed in Fig. 3a. At first, a piezopotential is created in ZnS by applied force owing to the non-centrosymmetric crystal structure of ZnS, especially around Mn^{2+} sites where local piezoelectric field could be higher. The generated piezopotential leads to the conduction band (CB) and valence band (VB) of ZnS tilting, which makes trapped

electrons possible to excite to CB. Then, these detrapped electrons recombine with holes by a non-radiation energy transfer. Meanwhile, the released energy may be transferred to Mn^{2+} ions, leading to their excitation. Finally, those excited Mn^{2+} ions will fall back to the ground state, $^4T_1$ (^4G)-$^6A_1$ (^6S), with the orange emission. Hence, it's clear that the strain-induced piezoelectric potential plays a crucial role in modifying the local band structure, and thus turns/controls the photon emission. Better yet, the ML intensity increases with the applied pressure, especially exhibiting a fine linear increasing trend in the range of 10-50 MPa, as shown in Fig. 3b [46].

Certainly, it should be clear that how the crystal structure, S vacancies, and doping concentration influence on the luminescent intensity to further verify the significant effect of piezopotential in this ML process of ZnS:Mn. Through optimizing technological parameters, different crystal structures of ZnS were obtained, and we found that wurtzite-type ZnS:Mn with a higher piezoelectric coefficient possessed distinctly stronger ML intensity than sphalerite ZnS:Mn, as displayed in Fig. 3c. Moreover, we developed a simple and available method for the oxygen-assisted preparation of ZnS:Mn, which could also effectively control the doping amount and deeply analyze the effects of S vacancies. As shown in Fig. 3d-e, the presence of O_2 has a positive influence on the formation of S vacancies, which cannot only generate more Mn^{2+} ions luminescent centers, but also create shallow donor levels, thus leading to the significant improvement of luminous efficiency [45, 46].

Additionally, this piezophotonic effect not just exists in those transition metal doped ZnS, but in many piezoelectric materials, such as CaZnOS, $SrAl_2O_4$, and $LiNbO_3$. As illustrated in Fig. 4a, we synthesized an Er-doped piezoelectric semiconductor CaZnOS:Er^{3+} [47]. It was

found that these particles not only have excellent mechanoluminescent properties with green light emission, but also possess outstanding temperature-sensitive upconversion luminescence characteristics ($^2H_{11/2}$, $^4S_{3/2} \rightarrow {}^4I_{15/2}$). Subsequently, we reported a lanthanide ions doped CaZnOS:Sm^{3+}, whose mechanoluminescent emissions are contributed to $^4G_{5/2} \rightarrow {}^6H_{5/2}$, $^4G_{5/2} \rightarrow {}^6H_{7/2}$, $^4G_{5/2} \rightarrow {}^6H_{9/2}$ and $^4G_{5/2} \rightarrow {}^6H_{11/2}$ f-f transitions of Sm^{3+}, as shown in Fig. 4b [48]. Moreover, Huang et al. systematically investigated the mechanisms of strain-induced emission in the transition metal-doped CaZnOS based on density functional theory [49]. Two primary luminous mechanisms are summarized: one is due to the formation of a deep or shallow energy trap induced by doped ions in the band gap, such as Cu-doping; another occurs by the energy transitions of doping ions from excited state to the ground state, such as Mn-doping.

To date, different kinds of mechanoluminescent materials have been known for over 400 years, but a complete unified discipline of this area has not yet formed [50-54]. Because, it still does not fully understand the underlying mechanism for a precise explanation of the mechanical-photonic energy conversion. But undoubtedly, piezopotential plays an important role to stimuli the light emission of certain materials. Especially for the nanogenerator and piezotronic materials with mechanically induced photon emission effect, they usually have a strong electron-lattice coupling effect. The external mechanical stimulus can be converted into the external electric field applied on these materials, which is a prerequisite for a self-recoverable material. Huang et al. summarized five dominant stages for the mechanically induced photon emission effect (Fig. 4c) [24]. The materials will firstly convert the external mechano-stimuli into equivalent electric-field as M-load mode noted. Then, the external

E-field induced electrical potential will be proportionally and directly converted into the energy-input. The gain in energy can further counteract the host for spatial-charge-separation of defects (Charging mode), which has been also confirmed from the electronic structures. This energy response and conversion can be accomplished within a short time or nearly simultaneous. When all responsible native defect complex is fulfilled the separation and charging, the systematic energy has been leveled up at the relative high energy. They will spontaneously experience a simultaneous process of agglomeration and de-charging. There are substantial amounts of energy released via the local lattice relaxation and support the electronic transitions between different levels along the paths of zero-phonon line. The corresponding energy will be released in forms of photon emissions (Release mode). Additionally, take the $LiNbO_3$ as an example, the system energy gains with external electric field applied. The magnitude of energy gains sufficiently covers and supports the neutrally paired intrinsic defect complex to experience the process of separation and de-charging (i.e. from A^+B^- to A^0B^0). This can be explained by the concept of charge alternation pair linked with the negative effective correlation energy (negative-U_{eff}). The charge alternation pairs (CAP) among the intrinsic point defects of host lattice are bounded excitions and can be stabilized by Coulomb potentials regardless the crossover distance. The inter-level hopping of electrons and holes between these CAP defects can be covered by the negative effective correlation energy (negative-U_{eff}) in order to overcome the barriers with equivalent life-time. The inter-level transitions of these charge carriers are actually along the zero-phonon-line of the electronic structures. Therefore, the intrinsic defects complex formed in CAP play a significant role in the electronic transitions for assisting the energy transfer through the

corresponding correlated pairs. During the past decade, MILE in piezoelectric materials has renewed great interest due to their application in smart sensors and energy saving illuminators. Better understanding the energy conversion mechanism for piezophotonic effect will help us establishing guidelines and a roadmap for developing and materializing the novel electro-optical technologies.

3 Device for Advanced Flexible Optoelectronic Applications Based on Piezophotonics

The piezophotonic effect is to use the piezopotential to trigger the carrier transport, recombination, and energy transfer for exciting the emission centers to emit photons under the dynamic mechanical stimulations. During the past decade, we are witnessing a rapid development of the research area of piezophotonics, and there are more and more state-of-the-art applications such as smart sensors and energy-saving illuminator and mechanical–optical–electric energy- interchangeable devices.

Different from the devices based on traditional electronics, the photon emission of the piezophotonic effect is directly triggered by mechanical force, such as bending, stretching, pinching, gliding and impact, without extra applying power. In the early days, when the phenomena being discovered, the stress luminescence was observed by scraping, rubbing or bumping. While the process of exerting stress is a reciprocating movement if consider a reversible application, the load of the luminescent body needs to be elastic and flexible. The mostly effective way to incorporate the particles and powders into a flexible or stretchable substrate. Organic elastomers with high transparency and high elasticity and scalability have been frequently used for piezophotonic devices, for instance, epoxy resin, polyethylene terephthalate (PET) and polydimethylsiloxane (PDMS) have been being used to incorporated

piezophotonic unite the in the flexible devices [55, 56].

3.1 Piezophotonic E-signature System

Recently, dramatically growing attention has been paid to digitalized feature recognition in human-machine interacting for information process security. E-signature is a type of intelligent data which contains signer's identity information in electronic form. It can provide users with authentication and body record easily and conveniently through the network. It also breaks through the limitation of time and space, and is commonly used in the fields of communication, electronic commerce, electronic government affairs and information security. At present, reliable electronic signatures protected by law have been widely used in daily life, such as handwritten signatures, private codes, personal codes, fingerprints, sounds, retinal structures and so on. Among them, handwritten digital signature is popular because of its convenience, which plays an irreplaceable role in the unique fields of digitalization, informatization and networking. However, as the threat of personal information security is becoming more and more serious, there is a huge challenge to the existing graphics and pattern processing technology which only records the handwriting of users. Therefore, searching for new human recognition feature information and exploring other details in the signature process are the most urgent problems in the field of information security.

Pressure sensor is the core component of handwritten e-signature device. Current technology can only record the user's handwritten graphics, while other information such as local pressure and writing speed in the signature process cannot be further recognized. Additionally, like fingerprints, sounds, retinas, etc. with personal characteristics, writing pressure and speed cannot be easily imitated by others, and thus used for authentication to

effectively prevent forgery and fraud. Therefore, these new sensors with personalized information will have a wide range of potential applications in artificial intelligence, electronic skin and other fields. At present, many research groups have developed high-performance novel pressure sensor arrays based on the change in capacitance, resistance and piezoelectricity. Nevertheless, these works are based on static force imaging, and the device requires a certain amount of energy consumption due to the electrical signal transmission. Hence, we developed a piezophotonic e-signature system which cannot only accurately image two-dimensional pressure distribution of dynamic stress in parallel, but also can directly convert the stress to an optical signal without applying extra power [45].

In this system, a charge-coupled device (CCD), as the image acquisition unit, is employed to obtain the information of the strain-induced photon emission; and a self-compiled soft program, as the signal processing unit, is used to carry out image processing for the real-time visible stress distribution, as illustrated in Fig. 5a. The device was constituted by packaging mechanoluminescent materials into two thin plastic protective films to form a sandwich structure (Fig. 5b). It's noted that those transparent polymeric films are benefit for the light transmission, and thus light can be observed on both sides of the device under applying pressure. Actually, both static pressure distribution and dynamic stress trajectory can be monitored and recorded by this system. By extracting the gray scale of the image, a two-dimensional distribution of light intensity is then acquired, which is related to the applied pressure, as shown in Fig. 4c. Indeed, this system is suitable for many kinds of mechanoluminescent materials with different light colors, such as ZnS:Cu [57], CaZnOS:Er^{3+} [47], CaZnOS:Sm^{3+} [48], as exhibited in Fig. 5d-f. A demonstration of signature

distinguishing via our system is presented in Fig. 5g, in which four processed signatures showing "*piezo*" signed by four people are listed together with their light intensity distribution map. It's obvious that the morphology and writing pressure of each signee are different. For instance, from the intensity distribution map, we can infer that the one who signed the signature (i) is used to write with a stronger force compared with the one signed signature (ii), and both of them intend to write steadily. In contrast, the third and fourth signees (iii & iv) are likely to write with a stronger force in some special stroke e.g. a sharp turn. In a word, the optical signals are pivotal for next-generation information technology instead of electrical signals, and more, unique and reliable personalized information can be obtained by using the piezophotonic e-signature system, such as the handwriting graphics, the applied local pressure/force and the signing speed. This landmark breakthrough in demonstration of newly designed static/dynamic pressure sensor matrix may enable unprecedented applications in pressure mapping, smart sensor networks, signature collections for high-level security systems, human/machine interface and artificial skins.

3.2 Stretchable Fibers and Wearable Electronic Devices

Recently, stretchable electronics have been paid more and more attention for the application in semiconductor devices, artificial intelligence, human-machine interaction. Recently, many research groups mixed the ML materials with elastic matrix to form stretchable fibers that could generate photon emission under elastic deformation. Jeong et al. first demonstrated a wind-driven ML device based on the stretchable fibers consisting of zinc supplied particles and PDMS, which possessed bright white ML and deep blue ML by using a gas flow system, as shown in Fig. 6a [58]. On the other hand, it's necessary to develop novel

synthetic techniques for the exploration of new practical applications based on these stretchable fibers. For instance, printings are great technologies for optic-electronic devices. As shown in Fig. 6b [59], Dinesh K. Patel et al. demonstrated a novel mechanoluminescent ink composing of ZnS particles, PDMS and a platinum curing retarder. Various kinds of complex 3 three-dimensional structures were designed by using a one-step 3D printing technology.

In particular, these light-emitting stretchable fibers have great potential applications for wearable electronic devices, with high-visibility property. Jeong et al. exhibited high-strength mechanoluminescent fibers consisting of PDMS and ZnS, which would generate photo emission under mechanical stimulation, such as stretching, twisting, as illustrated in Fig. 6c [60]. The structure of the fiber frame was investigated to enhance the adhesive force between the inorganic particles and elastic matrix. A demo of ML textile was then fabricated with high-visibility outfits. Additionally, Zhang et al. reported a highly stretchable ML fiber with different kinds of metal-doped zinc particles to turn the color of light emission, as shown in Fig. 6d [61]. The device also possessed excellent optical properties and stability after 10,000 cycles stretching and releasing.

3.3 Multi-physical Coupling Devices

Recently, multifunctional electronics are becoming more and more popular for their multiple-sensor integration. For ML materials, most of them also possess outstanding photoluminescence and electroluminescence properties. Jeong et al. demonstrated color-tunable composite film by changing the proportion of two different ML materials (ZnS:Cu,Mn and ZnS:Cu), as shown in Fig. 7a [62, 63]. By adding electrodes on each side of

the film, a bright electroluminescence phenomenon has been observed under an alternating current (AC). It was found that the frequency of AC and powder composition have great influence on the emission intensity and light colors. Additionally, by using patterning electrodes, different colors of light imaging could be acquired under applying an AC electric field and stress, as illustrated in Fig. 7b [64].

Furthermore, self-powered devices based on triboelectric nanogenerator (TENG) or the ML process are concerned in recent years, which can directly convert mechanical external force into an electrical signal without any power supplying. Since 2012, Wang group demonstrated many different kinds of TENGs, including vertical contact-separation mode, in-plane sliding mode, single-electrode mode and free-standing triboelectric-layer mode, which are all based on the coupling effect between contact electrification and electrostatic induction. In recent years, researchers have found that the sensor based on TENG has good pressure sensitivity, and thus a series of works have been reported on the high-resolution triboelectric sensor matrix for the real-time tactile mapping. Subsequently, we exhibited a stretchable triboelectric sensor with electric/light dual-mode based on the ZnS:Cu powder, as shown in Fig. 7c [65]. The device could convert the input mechanical stimuli to either electric or light output. Moreover, pressure sensitivity, measurement limit and pressure measurement range of the device are the key factors that determine the practical application of the device. Therefore, novel material systems or sensing mechanisms need to be further explored in order to obtain devices with adjustable pressure measurement range or full dynamic-range pressure sensor. Fortunately, the device integrated the two different sensing mechanisms discussed above could realize the full dynamic-range pressure detection and imaging [66]: the TENG

part covers the low-pressure regimes and the ML part takes over in the high-pressure regimes, as shown in Fig. 7d.

Moreover, the coupling effect between the strain-induced piezopotential and the magnetic-induced luminescence (MIL) has been gradually in the spotlight [67, 68]. In 2012, Hao's group exhibited a composite film with electric field-controllable luminescence, as shown in Fig. 8a [69]. A ZnS:Mn film was grown on the piezoelectric $Pb(Mg_{1/3}Nb_{2/3})O_3$-$x$$PbTiO_3$ (PMN-PT) substrate. It was found that the luminescence and ultrasound signal of the integrated film can be turned under an AC electric field owing to the converse piezoelectric effect in PMN-PT. Subsequently, they systematically investigated the MIL phenomenon by using a composite laminate system consisted of the metal-ion-doped ZnS as phosphor materials and a magnetic actuator, as illustrated in Fig. 8b [70]. Notably, the photo emission of the device can be tuned in reversible and dynamical manners even under a low magnetic field. Additionally, as shown in Fig. 8c, the magnetic excitation frequency has a major impact on the emission color of phosphor materials [71]. For the implementation of chip integration, a patterned single-crystal PMN-PT thin film was employed, and pixelated arrays with outstanding color tenability was then explored, as shown in Fig. 8c [72].

4 Advances in Piezophotonics materials and Future Trends

4.1 Novel Preparation process and Materials

Recent studies demonstrated milestone works in this field that piezo-oxides, oxy-sulfides, sulfides and niobate could be easily applied as high-performance mechanically induced photon emission materials through nano-engineering, either transition metal or rare earth ion doping, and achieved flexible color manipulations [73, 74]. The representatives are

shown in the Table 1. Reviewing the literatures, it can be found that the most frequently used piezophotonic semiconductor is transition metal doped ZnS which have two normal phases, blende and wurtzite structures ZnS, composing of Zn and S element. ZnS powders are the well-known phosphor. Recently, we reported an oxygen-assisted method for the preparation of wurtzite structured ZnS:Mn via high temperature solid-state reactions at normal pressure [46]. It's more biocompatible and environment friendly. It was found that the presence of O_2 could promote the introduction of sulfur vacancies, and thus increase the concentration of luminescence centers, resulting in the enhancement of the luminous intensity. Additionally, Gan and workers demonstrated a controlled hydrogenation method to fundamentally improve the ML performance of ZnS:Cu materials by introducing sulfur vacancies, the representative results for the mechanism and enhanced spectra, as showing in Fig. 9b [75].

As a new discovered piezoelectric semiconductor, CaZnOS shows intensively visible light emission under various mechanical energy stimuli by doping with transitional metals, such as Mn and Cu. As shown in Fig. 9c-d [76, 77], the latter also shows mechanical quenching properties. Beside visible emission, some lanthanide ions such Er and Nd doping materials show near infrared ML emission (Fig. 9e) [78]. Insulators are also found to show sensitive ML properties by using the piezoelectric effects. Tu and Xu reported a promising red-emitting piezoluminescence dietetic material that is achieved by doping rare earth Pr^{3+} into the well-known piezoelectric matrix, $LiNbO_3$. $Li_xNbO_3:Pr^{3+}$ exhibits unusually high piezoluminescence intensity as shown in Fig. 9f [79]. Interestingly, $Li_xNbO_3:Pr^{3+}$ shows excellent strain sensitivity at the lowest strain level, with no threshold for stress sensing. These multipiezo properties of sensitive piezoluminescence in a piezoelectric matrix possess

good performance, which are ideal for microstress sensing, damage diagnosis, electro-mechano-optical energy conversion, and multifunctional control in optoelectronics. Interestingly, Zhang reported a series of niobate that shows red emission, as shown in Fig. 9g [80], while previous work reported that dopants or non-doped niobate has green or blue color emission which might be due to the impurities. Additionally, piezophotonic materials are not only restricted in inorganic materials, they are also discovered in many organic complex.

4.2 Visual Electronic Skin

Electronic skin is a device that simulates human skin and senses complex surroundings through electronic technology. Like wearable devices, it has a variety of intelligent terminals. At present, there are many breakthroughs in the human simulation system. For example, the use of high-resolution cameras and high-fidelity sound system can replace human vision and voice. However, there are still many challenges to tactile sensors with high sensitivity and rapid response. In fact, as early as the 1970s, researchers began to focus on the application prospects of tactile sensing, and showed some inspiring touch sensors, such as artificial limbs with feedback systems and personal computer touchscreens. In the 1990s, flexible devices and stretchable devices are gradually becoming the hotspot. In just a few decades, high-performance pressure sensors based on different physical mechanisms have been reported. For example, transistor-based large-scale flexible sensor arrays not only have excellent mechanical and electrical properties, but also greatly reduce cross-talk between pixels in order to map pressure distributions more accurately.

Recently, visual electronic skin has brought a new hot research topic. Compared with electrical signals, optical signals are convenient for parallel fetch thus are increasingly

focused on and considered to be pivotal for next-generation information technology [81]. In our previous work, we have succeeded in fabricating an optical-based pressure sensor arrays based on the piezo-phototronic effect, as shown in Fig. 10a [82-86]. The device can image two-dimensional strain distribution in parallel, which is to use the inner-crystal piezopotential to tune the carrier separation, transport or recombination in optoelectronic processes. Additionally, Ali Javey's reported a user-interactive transistor matrix for pressure visualization based on organic light emitting diodes, as shown in Fig. 10b [87]. The luminescent intensity will enhance with the increasing pressure on the device, resulting in the visualization of pressure. Moreover, we also reported certain works on self-power large-scale, pressure-sensitive triboelectric sensor matrix for pressure imaging, as shown in Fig. 10c [88, 89].

In order to meet the needs of emerging areas including health monitoring, prosthetic limb technology and clinical medicine, it's urgent to obtain different types of artificial electronic skin with intelligent feedback system. Shepherd et al. reported an EL material consisting of transparent hydrogel electrodes and ZnS phosphor for stretchable displays, as shown in Fig. 11a [90]. By integrating the stretchable device with a soft robot, it can realize dynamic color tuning and sensory feedback under external and internal stimuli. In addition, Peng et al. demonstrated flexible and stretchable EL fibers, which can be used in dynamically textile displays of soft robotics, adjusting the color of textiles according to environmental changes, as exhibited in Fig. 11b [91]. Recently, Qian et al. systematically explored the effect of the elastic modulus on the ML properties of a flexible device. As shown in Fig. 11c [92], it was found that the luminescent intensity will change as long as there are tiny changes in

expression.

5 Conclusions

The research of piezophotonics and related area has been appreciated only in recent years when flexible optoelectronic became increasingly important. Materials with piezophotonic effect have mechanically induced light emission properties that can be stimulated by using a rather wide range of mechanical energy, including stretch, bending, friction, ultrasonic and wind, leading to highly flexible and operable properties. The ultimate aim of the piezophotonics is in the routine area of lighting, display and self-chargeable sensor and so on. In comparison with conventional bulk piezophotonic materials, small size of the particle would be resulted in some cutting-edge technologies such as high resolution stress imaging. Moreover, the deep fundamental mechanism from the energy band theory might be helpful for the mechanical-electrical-photonic energy conversion. All of those need scientific group from diverse areas.

In this review, we highly summarize the major advances in piezophotonic effect from the theoretical fundamental and practical applications. The strain-induced piezopotential can induce the photon emission without applying an external power. Generally, it's a common phenomenon on those piezoelectric mechanoluminescent materials, such as transition metal doped ZnS, CaZnOS, $SrAl_2O_4$, and $LiNbO_3$. Flexible/stretchable optoelectronic devices based on these mechanoluminescent materials were then widely investigated. More reliable personalized information can be achieved by using the piezophotonic e-signature system including the handwriting graphics and pressure distribution, which has great potential applications in high-level security systems. Different kinds of visible wearable electronic

devices and multi-physical coupling devices are also developed to to open up new using field for smart sensor networks, human/machine interface and artificial skins.

Acknowledgements

The authors express thanks for the support from the Natural Science Foundation of Beijing Municipality (2184131), the National Key R & D Project from the Minister of Science and Technology, China (2016YFA0202703), National Natural Science Foundation of China (Nos. 51622205, 61675027, 51432005, 61505010, 51502018, 51502018 and 61875136), Beijing Council of Science and Technology (Z171100002017019 and Z181100004418004), Natural Science Foundation of Beijing Municipality (Nos. 4181004, 4182080, 4184110), Shenzhen Fundamental Research Project (No. 000102), and Scientific Research Starting Foundation for the Youth Scholars of Shenzhen University (No. 000127).

References

[1] T. Rueckes, K. Kim, E. Joselevich, G.Y. Tseng, C.L. Cheung, C.M. Lieber, Science 289 (2000) 94.

[2] R.T. Tung, Mat. Sci. Eng. R. 35 (2001) 1.

[3] Y.W. Feng, L.L. Ling, Y.X. Wang, Z.M. Xu, F.L. Cao, H.X. Li, Z.F. Bian, Nano Energy 40 (2017) 481.

[4] Z.J. Pan, W.B. Peng, F.P. Li, Y.N. He, Nano Energy 49 (2018) 529.

[5] H.H. Singh, N. Khare, Nano Energy 51 (2018) 216.

[6] X.D. Wang, L. Dong, H.L. Zhang, R.M. Yu, C.F. Pan, Z.L. Wang, Adv. Sci. 2 (2015) 1500169.

[7] Z.L. Wang, J.H. Song, Science 312 (2006) 242.

[8] D.Q. Zheng, Z.M. Zhao, R. Huang, J.H. Nie, L.J. Li, Y. Zhang, Nano Energy 32 (2017) 448.

[9] F.P. Li, W.B. Peng, Z.J. Pan, Y.N. He, Nano Energy 48 (2018) 27.

[10] S. Qiao, J.H. Liu, G.S. Fu, K.L. Ren, Z.Q. Li, S.F. Wang, C.F. Pan, Nano Energy 49 (2018) 508.

[11] H.T. Liu, Q.L. Hua, R.M. Yu, Y.C. Yang, T.P. Zhang, Y.J. Zhang, C.F. Pan, Adv. Funct. Mater. 26 (2016) 5307.

[12] Q. Sun, D.H. Ho, Y. Choi, C. Pan, D.H. Kim, Z.L. Wang, J.H. Cho, ACS Nano 10 (2016) 11037.

[13] X. Han, W.M. Du, M.X. Chen, X.D. Wang, X.J. Zhang, X.Y. Li, J. Li, Z.C. Peng, C.F. Pan, Z.L. Wang, Adv. Mater. 29 (2017) 1701253.

[14] Y.F. Hu, C.F. Pan, Z.L. Wang, Semicond. Sci. Tech. 32 (2017) 053002.

[15] X.D. Wang, J.H. Song, J. Liu, Z.L. Wang, Science 316 (2007) 102.

[16] S. Xu, B.J. Hansen, Z.L. Wang, Nat. Commun. 1 (2010) 93.

[17] S. Xu, Y. Qin, C. Xu, Y.G. Wei, R.S. Yang, Z.L. Wang, Nat. Nanotech. 5 (2010) 366.

[18] G.A. Zhu, R.S. Yang, S.H. Wang, Z.L. Wang, Nano Lett. 10 (2010) 3151.

[19] Z.L. Wang, Adv. Mater. 19 (2007) 889.

[20] Z.Y. Gao, J. Zhou, Y.D. Gu, P. Fei, Y. Hao, G. Bao, Z.L. Wang, J. Appl. Phys. 106 (2009) 113707.

[21] Z.L. Wang, Mat. Sci. Eng. R. 64 (2009) 33.

[22] Y. Gao, Z.L. Wang, Nano Lett. 7 (2007) 2499.

[23] C.K. Jeong, K.I. Park, J. Ryu, G.T. Hwang, K.J. Lee, Adv. Funct. Mater. 24 (2014) 2620.

[24] B.L. Huang, M.Z. Sun, D.F. Peng, Nano Energy 47 (2018) 150.

[25] Y.Y. Peng, M.L. Que, J. Tao, X.D. Wang, J.F. Lu, G.F. Hu, B.S. Wan, Q. Xu, C.F. Pan, 2D Mater. 5 (2018) 042003.

[26] X.Q. Liu, X.N. Yang, G.Y. Gao, Z.Y. Yang, H.T. Liu, Q. Li, Z. Lou, G.Z. Shen, L. Liao, C.F. Pan, Z.L. Wang, ACS Nano 10 (2016) 7451.

[27] F. Xue, L.J. Yang, M.X. Chen, J. Chen, X.N. Yang, L.F. Wang, L.B. Chen, C.F. Pan, Z.L. Wang, Npg. Asia. Mater. 9 (2017) e418.

[28] M.L. Que, R.R. Zhou, X.D. Wang, Z.Q. Yuan, G.F. Hu, C.F. Pan, J .Phys-Condens. Mat. 28 (2016) 433001.

[29] R.R. Bao, C.F. Wang, Z.C. Peng, C. Ma, L. Dong, C.F. Pan, ACS Photonics 4 (2017) 1344.

[30] M.L. Que, X.D. Wang, Y.Y. Peng, C.F. Pan, Chinese Phys. B 26 (2017) 067301.

[31] Z.L. Wang, J. Phys. Chem. Lett. 1 (2010) 1388.

[32] Y. Qin, X.D. Wang, Z.L. Wang, Nature 451 (2008) 809.

[33] R.S. Yang, Y. Qin, L.M. Dai, Z.L. Wang, Nat. Nanotech. 4 (2009) 34.

[34] Z.L. Wang, R.S. Yang, J. Zhou, Y. Qin, C. Xu, Y.F. Hu, S. Xu, Mat. Sci. Eng. R. 70 (2010) 320.

[35] R.R. Bao, C.F. Wang, L. Dong, C.Y. Shen, K. Zhao, C.F. Pan, Nanoscale 8 (2016) 8078.

[36] M.X. Chen, C.F. Pan, T.P. Zhang, X.Y. Li, R.R. Liang, Z.L. Wang, ACS Nano 10 (2016)

6074.

[37] Z.L. Wang, Nano Today 5 (2010) 540.

[38] Z.L. Wang, Adv. Funct. Mater. 18 (2008) 3553.

[39] Z.L. Wang, Adv. Mater. 24 (2012) 4632.

[40] C.R. Crowell, S.M. Sze, Solid-State Electron. 9 (1966) 1035.

[41] L.J. Brillson, Y.C. Lu, J. Appl. Phys. 109 (2011) 121301.

[42] Y.F. Hu, Y. Zhang, C. Xu, G.A. Zhu, Z.L. Wang, Nano Lett. 10 (2010) 5025.

[43] K. Momeni, G.M. Odegard, R.S. Yassar, J. Appl. Phys. 108 (2010) 114303.

[44] A.N. Morozovska, E.A. Eliseev, S.V. Svechnikov, A.D. Krutov, V.Y. Shur, A.Y. Borisevich, P. Maksymovych, S.V. Kalinin, Phys. Rev. B 81 (2010).

[45] X.D. Wang, H.L. Zhang, R.M. Yu, L. Dong, D.F. Peng, A.H. Zhang, Y. Zhang, H. Liu, C.F. Pan, Z.L. Wang, Adv. Mater. 27 (2015) 2324.

[46] X.D. Wang, R. Ling, Y.F. Zhang, M.L. Que, Y.Y. Peng, C.F. Pan, Nano Res. 11 (2018) 1967.

[47] H.L. Zhang, D.F. Peng, W. Wang, L. Dong, C.F. Pan, J. Phys. Chem. C 119 (2015) 28136.

[48] W. Wang, D.F. Peng, H.L. Zhang, X.H. Yang, C.F. Pan, Opt. Commun. 395 (2017) 24.

[49] B.L. Huang, D.F. Peng, C.F. Pan, Phys. Chem. Chem. Phys. 19 (2017) 1190.

[50] B.P. Chandra, C.N. Xu, H. Yamada, X.G. Zheng, J. Lumin. 130 (2010) 442.

[51] C.N. Xu, T. Watanabe, M. Akiyama, X.G. Zheng, Appl. Phys. Lett. 74 (1999) 1236.

[52] C.N. Xu, T. Watanabe, M. Akiyama, X.G. Zheng, Appl. Phys. Lett. 74 (1999) 2414.

[53] X.S. Wang, C.N. Xu, H. Yamada, K. Nishikubo, X.G. Zheng, Adv. Mater. 17 (2005)

1254.

[54] C.N. Xu, H. Yamada, X.S. Wang, X.G. Zheng, Appl. Phys. Lett. 84 (2004) 3040.

[55] G.F. Hu, W.X. Guo, R.M. Yu, X.N. Yang, R.R. Zhou, C.F. Pan, Z.L. Wang, Nano Energy 23 (2016) 27.

[56] F. Li, X.D. Wang, Z.G. Xia, C.F. Pan, Q.L. Liu, Adv. Funct. Mater. 27 (2017) 1700051.

[57] X.Y. Wei, X.D. Wang, S.Y. Kuang, L. Su, H.Y. Li, Y. Wang, C.F. Pan, Z.L. Wang, G. Zhu, Adv. Mater. 28 (2016) 6656.

[58] S.M. Jeong, S. Song, K.I. Joo, J. Kim, S.H. Hwang, J. Jeong, H. Kim, Energy Environ. Sci. 7 (2014) 3338.

[59] D.K. Patel, B.-E. Cohen, L. Etgar, S. Magdassi, Mater. Horiz. 5 (2018) 708.

[60] S.M. Jeong, S. Song, H.-J. Seo, W.M. Choi, S.-H. Hwang, S.G. Lee, S.K. Lim, Adv. Sustainable Syst. 1 (2017) 1700126.

[61] J. Zhang, L.K. Bao, H.Q. Lou, J. Deng, A. Chen, Y.J. Hu, Z.T. Zhang, X.M. Sun, H.S. Peng, J. Mater. Chem. C 5 (2017) 8027.

[62] S.M. Jeong, S. Song, S.K. Lee, N.Y. Ha, Adv. Mater. 25 (2013) 6194.

[63] S.M. Jeong, S. Song, S.K. Lee, B. Choi, Appl. Phys. Lett. 102 (2013) 051110.

[64] S.M. Jeong, S. Song, H. Kim, Nano Energy 21 (2016) 154.

[65] H.J. Fang, X.D. Wang, Q. Li, D.F. Peng, Q.F. Yan, C.F. Pan, Adv. Energy Mater. 6 (2016) 1600829.

[66] X.D. Wang, M.L. Que, M.X. Chen, X. Han, X.Y. Li, C.F. Pan, Z.L. Wang, Adv. Mater. 29 (2017) 1605817.

[67] Y. Zhang, W.J. Jie, P. Chen, W.W. Liu, J.H. Hao, Adv. Mater. 30 (2018) 1707007.

[68] L. Chen, M.C. Wong, G.X. Bai, W.J. Jie, J.H. Hao, Nano Energy 14 (2015) 372.

[69] Y. Zhang, G.Y. Gao, H.L.W. Chan, J.Y. Dai, Y. Wang, J.H. Hao, Adv. Mater. 24 (2012) 1729.

[70] M.C. Wong, L. Chen, M.K. Tsang, Y. Zhang, J.H. Hao, Adv. Mater. 27 (2015) 4488.

[71] M.C. Wong, L. Chen, G.X. Bai, L.B. Huang, J.H. Hao, Adv. Mater. 29 (2017) 1701945.

[72] Y. Chen, Y. Zhang, D. Karnaushenko, L. Chen, J.H. Hao, F. Ding, O.G. Schmidt, Adv. Mater. 29 (2017) 1605165.

[73] C. Pan, J.C. Zhang, M. Zhang, X. Yan, Y.Z. Long, X.S. Wang, Appl. Phys. Lett. 110 (2017) 233904.

[74] D. Peng, B. Chen, F. Wang, ChemPlusChem 80 (2015) 1209.

[75] J.Y. Gan, M.G. Kang, M.A. Meeker, G.A. Khodaparast, R.J. Bodnar, J.E. Mahaney, D. Maurya, S. Priya, J. Mater. Chem. C 5 (2017) 5387.

[76] D. Tu, C.N. Xu, Y. Fujio, A. Yoshida, Light-Sci. Appl. 4 (2015) e356.

[77] J.C. Zhang, L.Z. Zhao, Y.Z. Long, H.D. Zhang, B. Sun, W.P. Han, X. Yan, X.S. Wang, Chem. Mater. 27 (2015) 7481.

[78] L.J. Li, L. Wondraczek, L.H. Li, Y. Zhang, Y. Zhu, M.Y. Peng, C.B. Mao, ACS Appl. Mater. Interfaces 10 (2018) 14509.

[79] D. Tu, C.N. Xu, A. Yoshida, M. Fujihala, J. Hirotsu, X.G. Zheng, Adv. Mater. 29 (2017) 1606914.

[80] J.C. Zhang, Y.Z. Long, X. Yan, X.S. Wang, F. Wang, Chem. Mater. 28 (2016) 4052.

[81] Y. Kim, J.-S. Kim, G.-W. Kim, Sci. Rep. 8 (2018) 12023.

[82] C.F. Pan, L. Dong, G. Zhu, S.M. Niu, R.M. Yu, Q. Yang, Y. Liu, Z.L. Wang, Nat.

Photonics 7 (2013) 752.

[83] X. Han, M.X. Chen, C.F. Pan, Z.L. Wang, J. Mater. Chem. C 4 (2016) 11341.

[84] C.F. Pan, M.X. Chen, R.M. Yu, Q. Yang, Y.F. Hu, Y. Zhang, Z.L. Wang, Adv. Mater. 28 (2016) 1535.

[85] X.F. Wang, W.B. Peng, C.F. Pan, Z.L. Wang, Semicond. Sci. Tech. 32 (2017) 043005.

[86] L.P. Zhu, L.F. Wang, C.F. Pan, L.B. Chen, F. Xue, B.D. Chen, L.J. Yang, L. Su, Z.L. Wang, ACS Nano 11 (2017) 1894.

[87] C. Wang, D. Hwang, Z.B. Yu, K. Takei, J. Park, T. Chen, B.W. Ma, A. Javey, Nat. Mater. 12 (2013) 899.

[88] X.D. Wang, H.L. Zhang, L. Dong, X. Han, W.M. Du, J.Y. Zhai, C.F. Pan, Z.L. Wang, Adv. Mater. 28 (2016) 2896.

[89] X.D. Wang, Y.F. Zhang, X.J. Zhang, Z.H. Huo, X.Y. Li, M.L. Que, Z.C. Peng, H. Wang, C.F. Pan, Adv. Mater. 30 (2018) 1706738.

[90] C. Larson, B. Peele, S. Li, S. Robinson, M. Totaro, L. Beccai, B. Mazzolai, R. Shepherd, Science 351 (2016) 1071.

[91] Z.T. Zhang, L.Y. Cui, X. Shi, X.C.R. Tian, D.P. Wang, C.N. Gu, E. Chen, X.L. Cheng, Y.F. Xu, Y.J. Hu, J.Y. Zhang, L. Zhou, H.H. Fong, P.B. Ma, G.M. Jiang, X.M. Sun, B. Zhang, H.S. Peng, Adv. Mater. 30 (2018) 1800323.

[92] X. Qian, Z.R. Cai, M. Su, F.Y. Li, W. Fang, Y.D. Li, X. Zhou, Q.Y. Li, X.Q. Feng, W.B. Li, X.T. Hu, X.D. Wang, C.F. Pan, Y.L. Song, Adv. Mater. 30 (2018) 1800291.

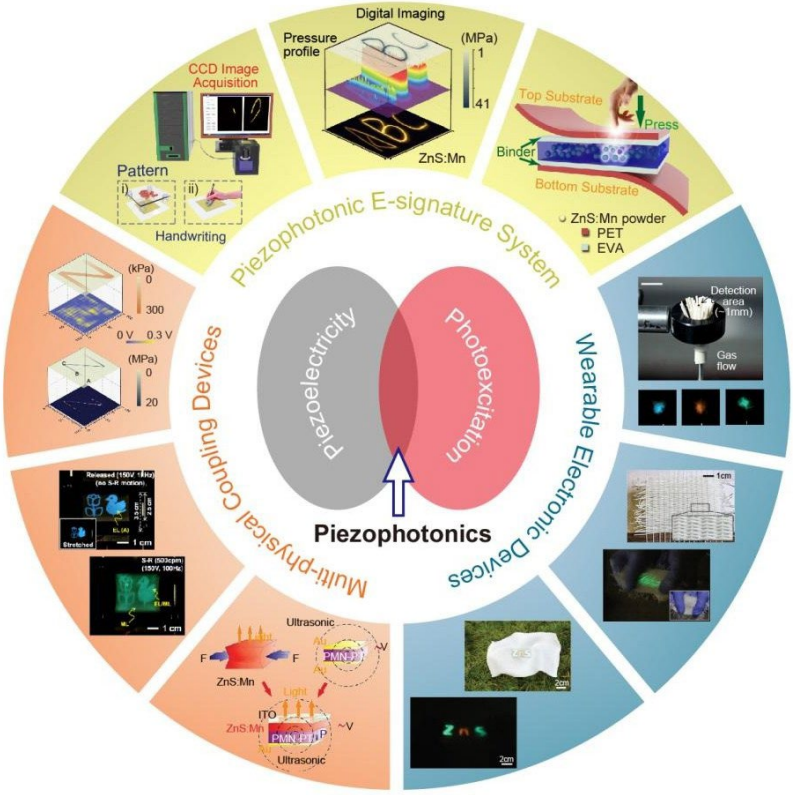

Fig. 1. Scheme of piezophotonics and recently developed devices for advanced flexible optoelectronic applications. “Piezophotonic e-signature system” [45, 46], (Reproduced with permission. Copyright 2015, Wiley VCH; Copyright 2018, Springer Nature); “Wearable electronic devices” [58, 60, 61], (Reproduced with permission. Copyright 2014, Royal Society of Chemistry; Copyright 2017, Wiley VCH; Copyright 2017, Royal Society of Chemistry); “Multi-physical coupling devices” [64, 66, 69], (Reproduced with permission. Copyright 2016, Elsevier Ltd.; Copyright 2017, Wiley VCH; Copyright 2012, Wiley VCH).

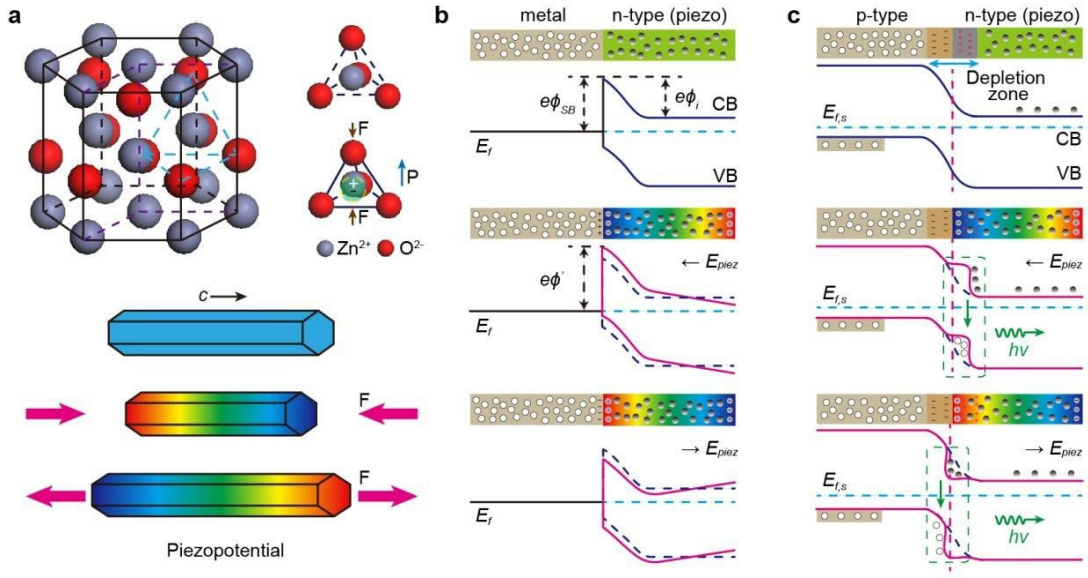

Fig. 2. (a) Atomic structure ZnO. Numerical calculation of the piezoelectric potential distribution along a ZnO nanowire under axial strain [39]. (Reproduced with permission. Copyright 2012, Wiley VCH). (b-c) Piezotronic effect on the M-S interface and the p-n junction [37]. (Reproduced with permission. Copyright 2010, Elsevier Ltd.).

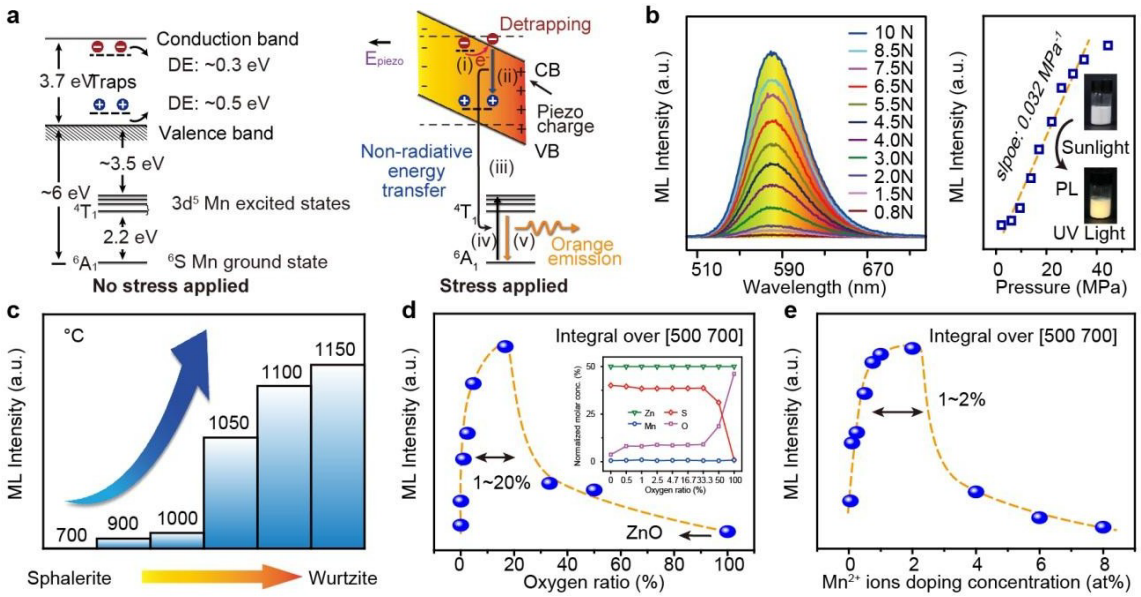

Fig. 3. (a) Schematic illustration of band diagram of Mn-doped ZnS and the piezophotonic effect initiated the ML process due to the strain-induced piezo-potential facilitate the detrapping of electrons [45]. (b-e) ML spectra under different applied forces [45, 46]. (Reproduced with permission. Copyright 2015, Wiley VCH; Copyright 2018, Springer Nature).

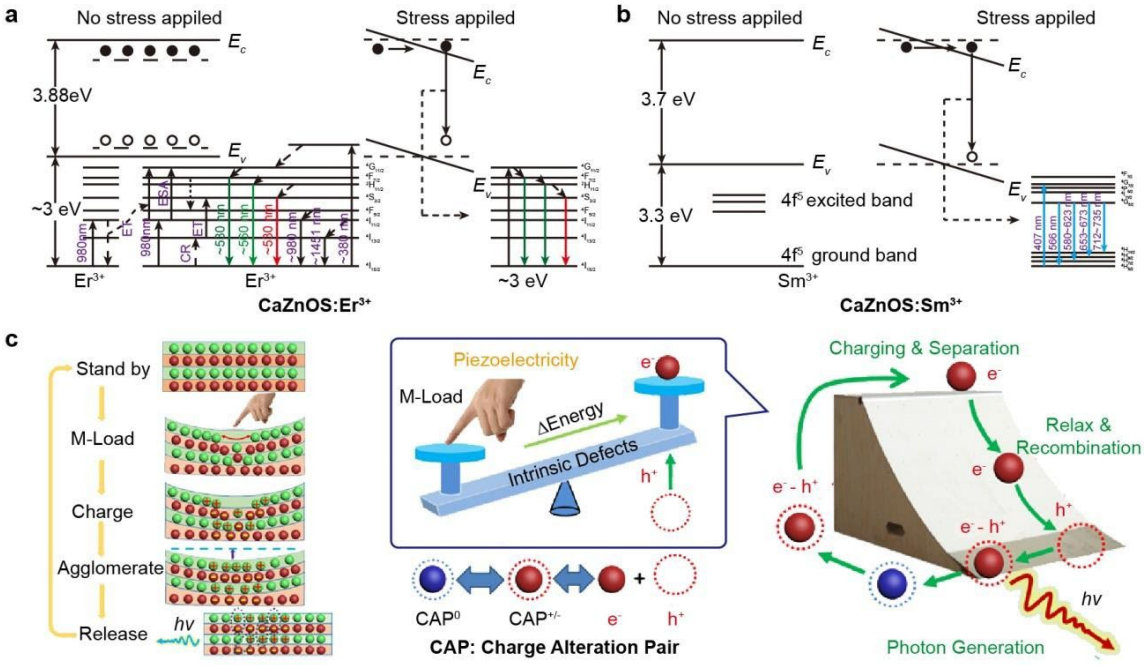

Fig. 4. (a) ML processes in the Er^{3+} doped CaZnOS [47]. (Reproduced with permission. Copyright 2015, American Chemical Society). (b) Mechanical-induced emission in the Sm^{3+} doped CaZnOS [48]. (Reproduced with permission. Copyright 2017, Elsevier Ltd.). (c) Schematic diagram of the native defects and energy conversion process [24]. (Reproduced with permission. Copyright 2018, Elsevier Ltd.).

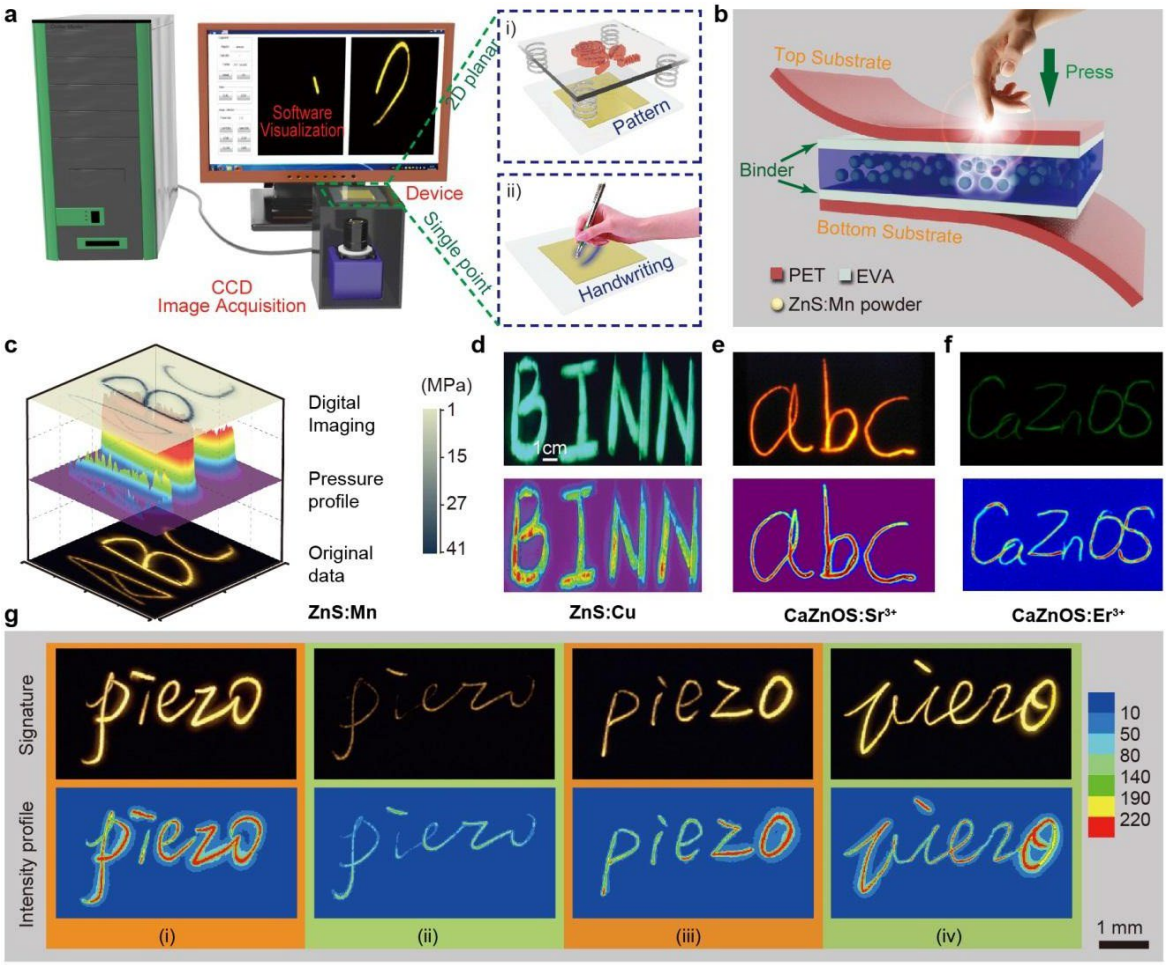

Fig. 5. (a-b) Schematic illustration of the device and the image acquisition and processing system [45]. (Reproduced with permission. Copyright 2015, Wiley VCH). (c-f) Pressure mapping based on ZnS:Mn, ZnS:Cu, CaZnOS:Sr^{3+}, CaZnOS:Er^{3+}, respectively [46-48, 57]. (Reproduced with permission. Copyright 2018, Springer Nature; Copyright 2016, Wiley VCH; Copyright 2015, American Chemical Society; Copyright 2017, Elsevier Ltd.). (g) Demonstrations of recording the signing habits of four signees by PSM devices under different signature pressure [45]. (Reproduced with permission. Copyright 2015, Wiley VCH).

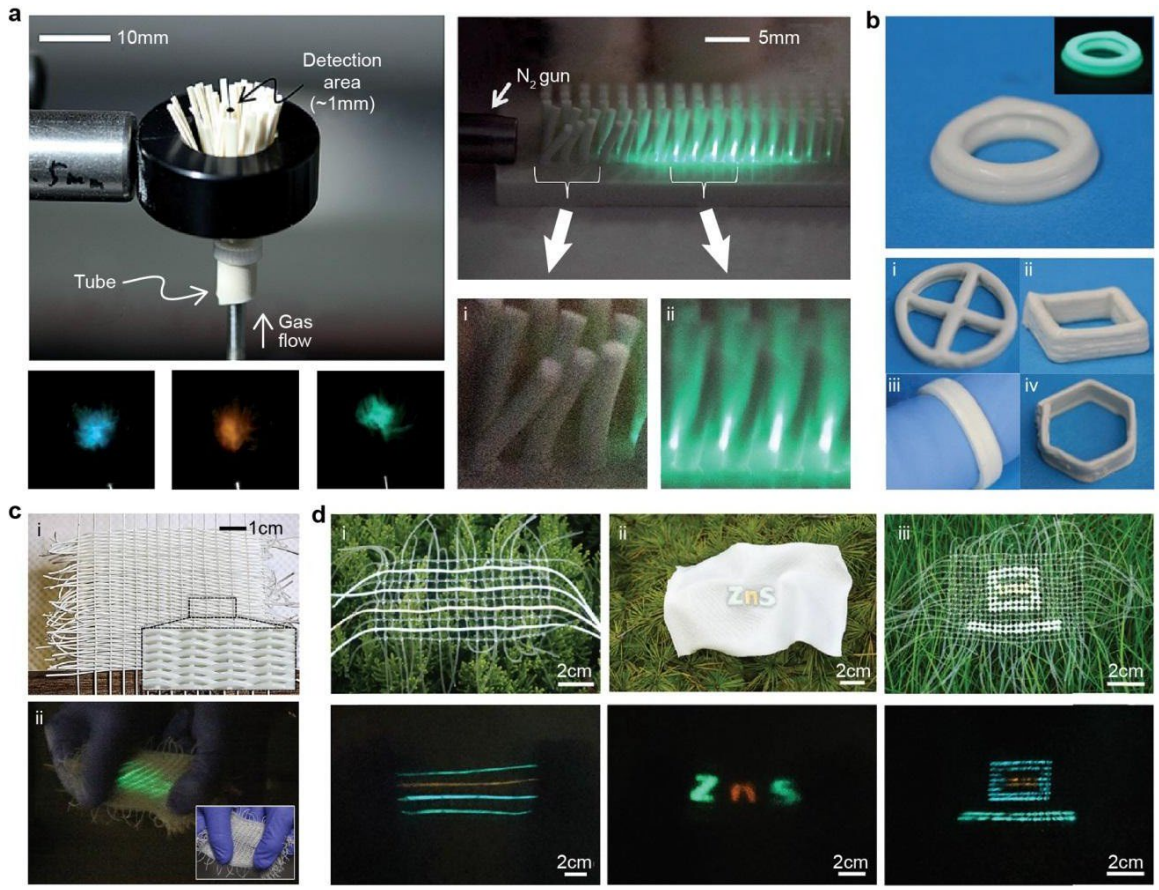

Fig. 6. (a) Photograph of a partially sliced ML composite enclosed by a ring holder which will come about different color under different gas flow [58]. (Reproduced with permission. Copyright 2014, Royal Society of Chemistry). (b) 3D printed ML candy, and a ring with a plus at the center, a hollow square, a ring, and a hollow hexagon [59]. (Reproduced with permission. Copyright 2018, Royal Society of Chemistry). (c) Photograph of hand-loomed prototype of ML fabric [60]. (Reproduced with permission. Copyright 2017, Wiley VCH). (d) Photographs of the mechanoluminescent fabrics based on mechanoluminescent fibers, ribbons and dots [61]. (Reproduced with permission. Copyright 2017, Royal Society of Chemistry).

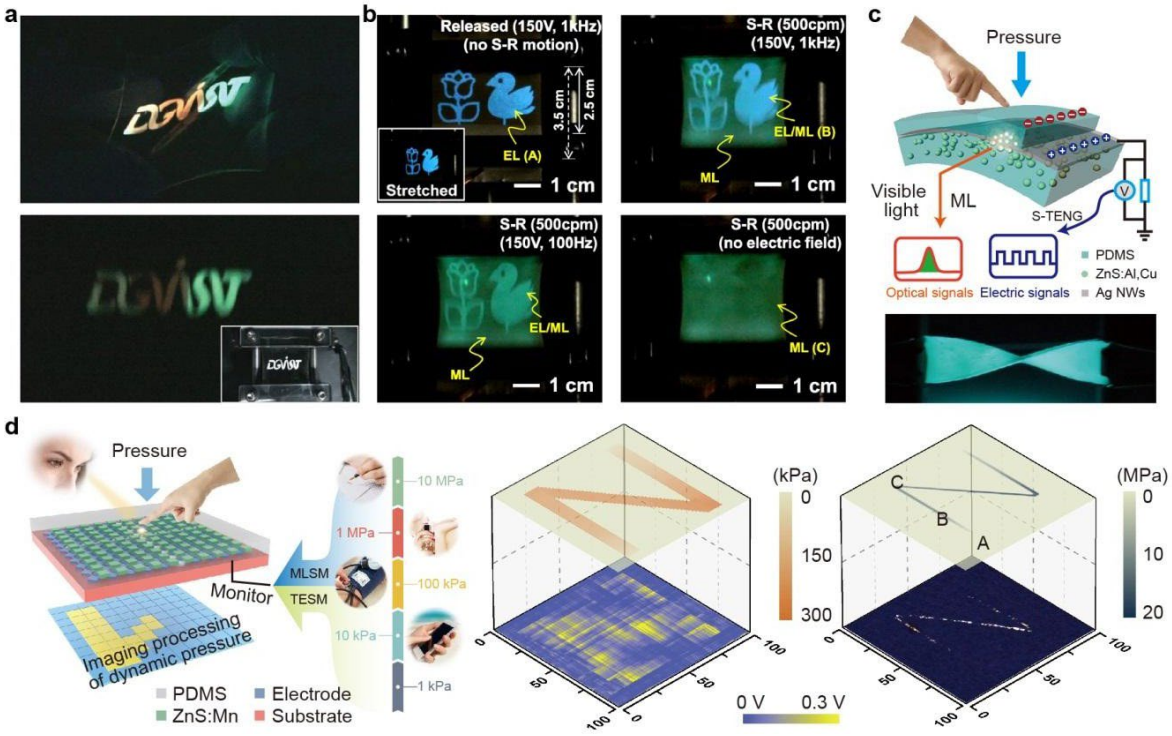

Fig. 7. (a) Photographs of the photoluminescent and mechanoluminescent patterned composite film with three different colors: yellow, orange, and green [62]. (Reproduced with permission. Copyright 2013, Wiley VCH). (b) Photographs of the patterned EL, EL/ML and ML images under various electro-mechanical stress conditions [64]. (Reproduced with permission. Copyright 2016, Elsevier Ltd.) (c) Working principle of the stretchable nanogenerator with optical/electrical dual-mode [65]. (Reproduced with permission. Copyright 2016, Wiley VCH). (d) Illustration of the pressure mapping process by using full dynamic-range pressure sensor arrays [66]. (Reproduced with permission. Copyright 2017, Wiley VCH).

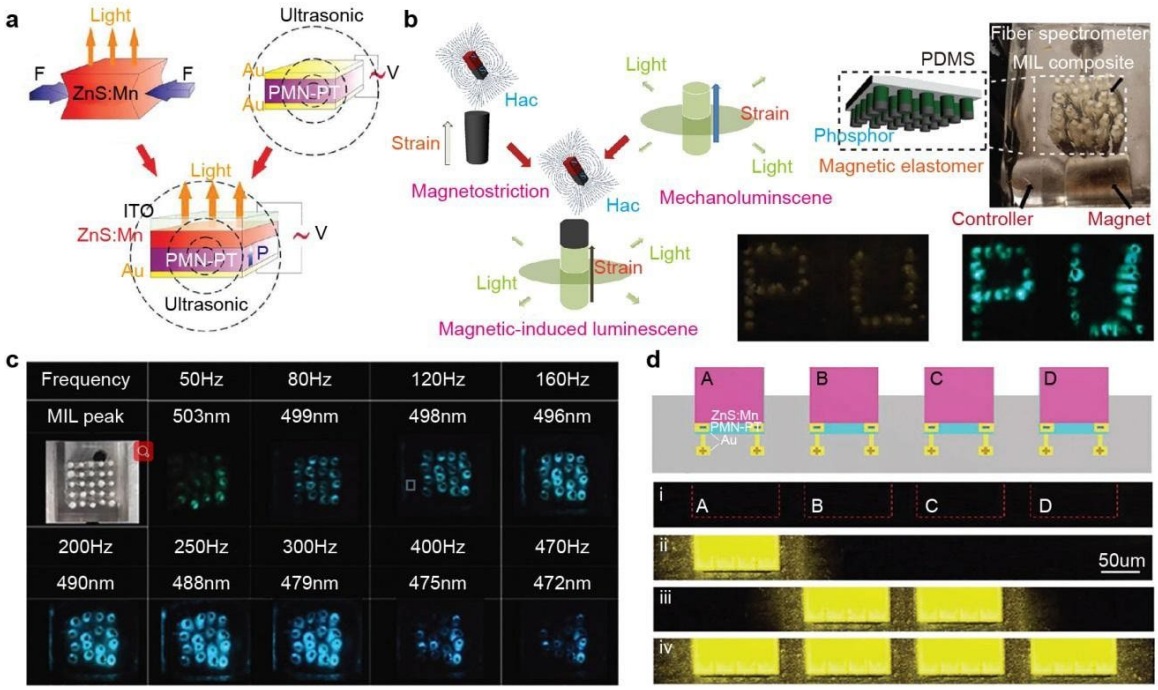

Fig. 8. (a) The procedure used for measuring the luminescent and ultrasonic characteristics of ZnS:Mn film grown on PMN–PT substrate under an AC electric-field [69]. (Reproduced with permission. Copyright 2012, Wiley VCH). (b) Implementation of MIL effect based on strain-mediated magnetoluminescent coupling in two phases of magnetic elastomer and mechanoluminescence phosphor [70]. (Reproduced with permission. Copyright 2015 Wiley VCH). (c) Integrated emission intensity as a function of the modulation frequency of the magnetic field at fixed strength [71]. (Reproduced with permission. Copyright 2017 Wiley VCH). (d) Demonstration of four representative addressable light emission states is shown on the bottom photographs [72]. (Reproduced with permission. Copyright 2017 Wiley VCH).

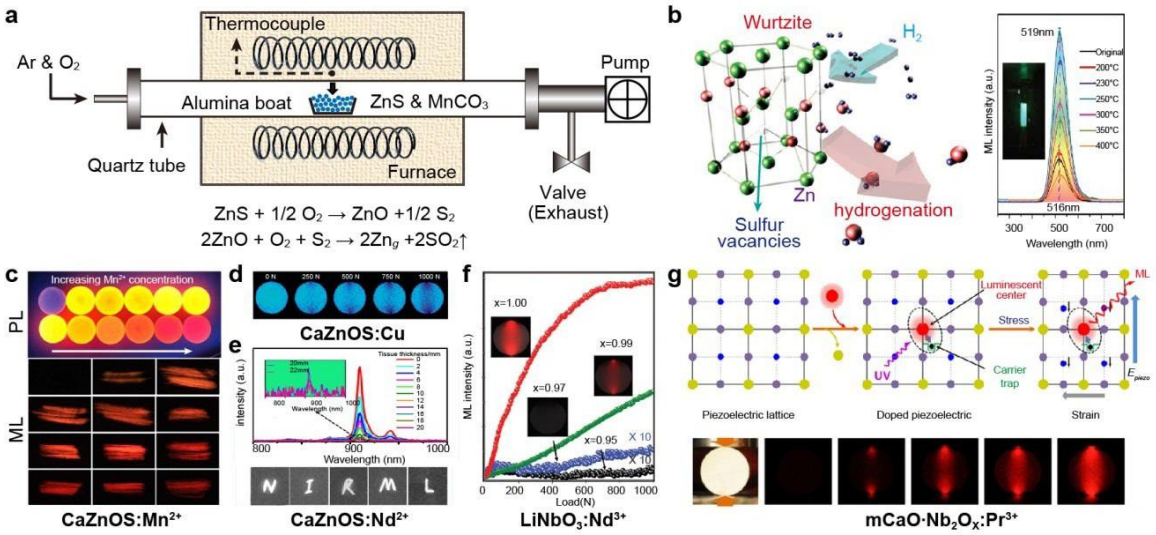

Fig. 9. (a) Preparation of mechanoluminescent ZnS:Mn with oxygen assistance [46]. (Reproduced with permission. Copyright 2018, Springer Nature). (b) Conceptual description for synthesizing defect-modified non-stoichiometric particles using the hydrogenation technique [75]. (Reproduced with permission. Copyright 2017 Royal Society of Chemistry). (c) Color manipulation of PL and ML from CaZnOS:Mn by different Mn^{2+} concentration effect [77]. (Reproduced with permission. Copyright 2015 American Chemical Society). (d) ML properties of CaZnOS:Cu under different load pressure [76]. (Reproduced with permission. Copyright 2015 Springer Nature). (e) Emission spectra of CaZnOS:Nd^{3+} passing through the tissues with different thicknesses [78]. (Reproduced with permission. Copyright 2018 American Chemical Society). (f) Comparison of ML intensities for $Li_xNbO_3:Pr^{3+}$ with different x values [79]. (Reproduced with permission. Copyright 2017 Wiley VCH). (g) Schematic illustration of the design strategy to create recoverable ML in piezoelectrics and recoverable ML in Pr^{3+} activated calcium niobate systems [80]. (Reproduced with permission. Copyright 2016 American Chemical Society).

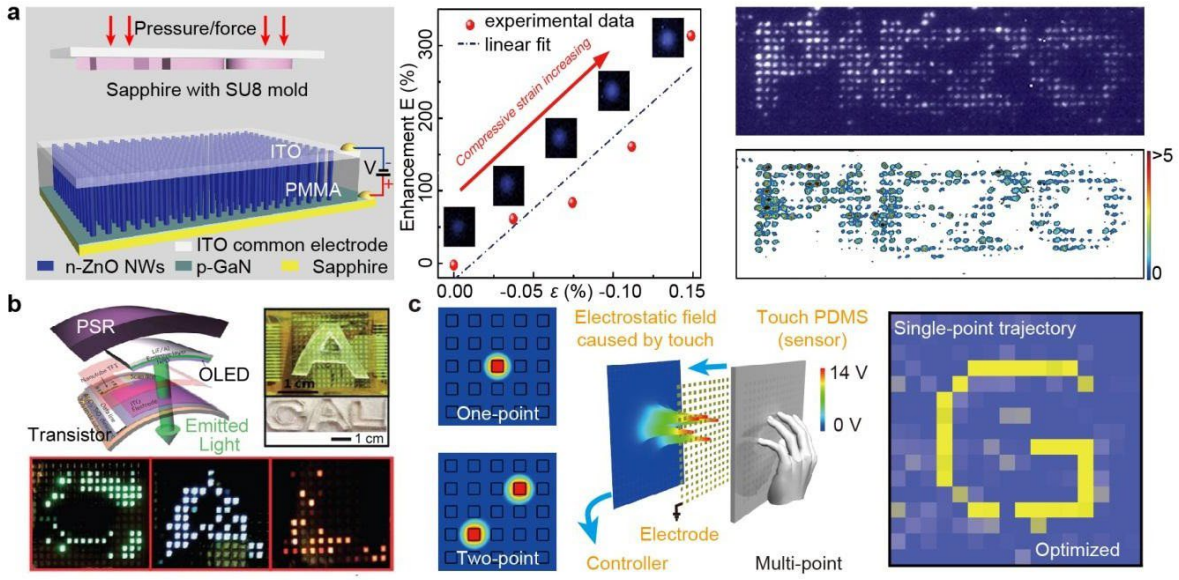

Fig. 10. (a) Schematical device design for imaging pressure distribution using the piezophototronic effect. Optical image of the device with a convex mould on top is shown on the right [82]. (Reproduced with permission. Copyright 2013 Springer Nature). (b) Large-scale transistor matrix for pressure visualization based on organic light emitting diodes [87]. (Reproduced with permission. Copyright 2013 Springer Nature). (c) Self-powered triboelectric tactile sensor matrix for rapid tactile mapping [88]. (Reproduced with permission. Copyright 2016, Wiley-VCH).

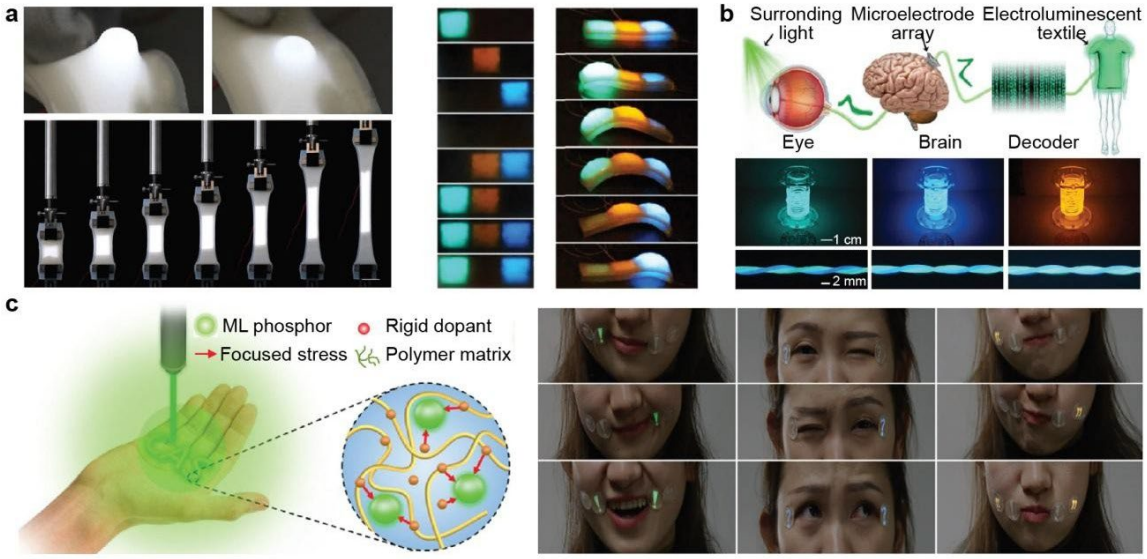

Fig. 11. (a) EL material consisting of transparent hydrogel electrodes and ZnS phosphor for stretchable displays [90]. (Reproduced with permission. Copyright 2017 American Association for the Advancement of Science). (b) Schematic showing the use of flexible and stretchable EL fibers for a brain-interfaced camouflage system [91]. (Reproduced with permission. Copyright 2018 Wiley VCH) (c) Skin-driven various color ML response to lips corner, canthus, and cheek muscle movements [92]. (Reproduced with permission. Copyright 2018 Wiley VCH)

Table 1. Typical piezophotonic materials

Piezophotonic host	Dopant	Color	Ref.
ZnS	Cu/Mn	Green/red	[45, 46, 62]
CaZnOS	Cu/Mn/Sm,Er,Nd	Blue/green/red/near infrared	[47, 76]
$LiNbO_3$/$NaNbO_3$	Pr	Red	[79]